Japanese Journal of
Applied Physics

Oxygen Vacancy Chain Formation in TiO_2 under External Strain for Resistive Switching Memory

Japanese Journal of Applied Physics **51** (2012) 06FG14 **REGULAR PAPER**
DOI: 10.1143/JJAP.51.06FG14

Oxygen Vacancy Chain Formation in TiO_2 under External Strain for Resistive Switching Memory

Dong Su Yoo, Kiyong Ahn, Sung Beom Cho, Minho Lee, and Yong-Chae Chung*

Department of Materials Science and Engineering, Hanyang University, Seoul 133-791, Republic of Korea

Received November 30, 2011; accepted January 7, 2012; published online June 20, 2012

The electronic structure and vacancy formation energy of rutile TiO_2 with ordered oxygen vacancies were calculated using the density functional theory with on-site Coulomb corrections between Ti 3d orbital and O 2p orbital (LDA+U^d+U^p). The calculated band gaps are about 3 eV, using LDA+U^d+U^p, and a hybrid functional proposed by Heyd–Scuseria–Ernzerhog. The ordered oxygen vacancies were introduced along the [001] direction within a 3×3×4 supercell of rutile TiO_{2-x} that consisted of 72 Ti and 136 O atoms. Biaxial strain was induced in the rutile TiO_2 along the *x*- and *y*-directions up to ±5%. The lowest formation energy of ordered oxygen vacancies was found in 5% compressive strain and deemed as a thermodynamically favorable structure.

1. Introduction

Resistive random access memory (ReRAM) is becoming increasingly promising for next-generation nonvolatile memory due to its properties of high density, low operating power, fast switching speed, and compatibility with the conventional complementary metal–oxide–semiconductor process. Recently, resistance switching materials, such as TiO_2, NiO, Al_2O_3, $SrTiO_3$, PrCaMnO, and Cu_2S, have been investigated to show memristive switching behavior.[1–6] Moreover, TiO_2 also has an outstanding memristive switching behavior which leads to a great research interest in the properties of ReRAM.[7]

The oxygen defects in the bulk and the interface are believed to play a critical role in the memristive switching behavior.[8] There have been several attempts to explain the memristive switching behavior using the charge trapping model, the conductive filament formation model, the Schottky barrier modulation model and the electrochemical migration of point defects.[9–12] However, these models cannot completely explain the switching mechanism. Recently, direct observation of an oxygen vacancy chain of TiO_2 using high-resolution transmission electron microscopy has been reported.[13] Moreover, Park *et al.* reported the first-principles calculation for the electronic properties of rutile TiO_2 with ordered oxygen vacancies showing a transition from a resistive to conductive oxide as a function of vacancy ordering. It was also proposed that the lowest formation energy is observed in the vacancy chain along the [001] direction, suggesting that the structure of TiO_2 with a vacancy chain is the most favorable structure.[14]

In the fabrication of nanostructures and thin films, external strain effect is inevitable.[15,16] Interplay between external strain and oxygen vacancies on TiO_2 play important roles on the surfaces and in the bulk.[17,18] The strain effect also comes as a new method to tuning the band gap of TiO_2.[19,20]

Therefore, considering the strain effect, more accurate calculations for atomic and electronic structures based on the density functional theory (DFT) of ordered oxygen vacancies are necessary to elucidate, from a theoretical viewpoint, its influence on the resistive switching mechanism.

Generally, DFT methods are well known for reasonably obtaining structural properties, such as lattice parameters and bulk modulus. However, for the representation of the electronic properties of semiconductors, such as band gaps and effective masses, DFT gives unsatisfactory calculation results. Therefore, DFT + green function with screened coulomb interaction or exact-exchange DFT calculation methods are used for prediction of high precision band gap.[21,22] However, these methods are computationally heavy; to apply these methods to large systems like a 3×3×4 supercell of TiO_2, which have 1728 valence electrons, seems to be difficult. Therefore, to obtain a more accurate electronic structure of TiO_2, a LDA with the addition of on-site Coulomb corrections (LDA+U) method was performed.

In this work, electronic properties and thermodynamically favorable structures with the ordered oxygen vacancies along the [001] direction are computed in the 3×3×4 TiO_2 and TiO_{2-x} supercell systems with LDA+U.

2. Calculation Method

The spin polarized first-principle calculations were performed using density functional theory with the LDA+U method[23] for the description of the exchange and correlation energy of electrons. Using the Vienna *ab initio* simulation package (VASP) code,[24] the self-consistent electronic density functional and the total energy were calculated with a projector augmented wave.[25] The plane-wave basis was set to expand to a cutoff energy of 353.0 eV (25.95 Ry). The self-consistent loop was iterated until the total energy difference of systems between the adjacent iterating steps became less than 10^{-6} eV. All atoms in the TiO_2 and TiO_{2-x} systems were fully relaxed for structural optimization until the maximum Hellmann–Feynman forces were in the range of ±0.005 eV/Å.[26] The ionic relaxation is based on the conjugate gradient method.[27] The nonshifted Monkhorst–Pack scheme of 2×2×2 k-point grids is used for Brillouin zone sampling.[28] A pseudoatomic calculation was performed with Ti $3s^2 3p^6 3d^2 4s2$ and O $2s^2 2p^4$ states of valence electrons.

The Heyd–Scuseria–Ernzerhog (HSE) hybrid functional (HF) was implemented in the present work, which employs a screened short-range HF exchange instead of a full exact HF exchange.[29] The exchange-correlation energy is defined as

$$E_{xc}^{HSE} = E_x^{DFT} - \frac{1}{4} E_x^{DFT,SR}(\mu) + \frac{1}{4} E_x^{HF,SR}(\mu) + E_C^{DFT}, \quad (1)$$

*E-mail address: yongchae@hanyang.ac.kr

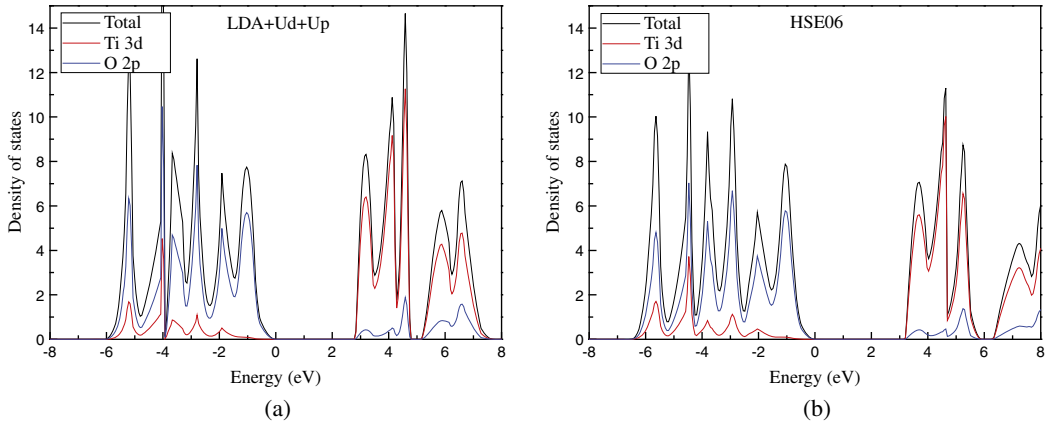

Fig. 1. (Color online) Density of states (DOS) of a TiO_2 unit cell using (a) LDA+U^d+U^p and (b) HSE06.

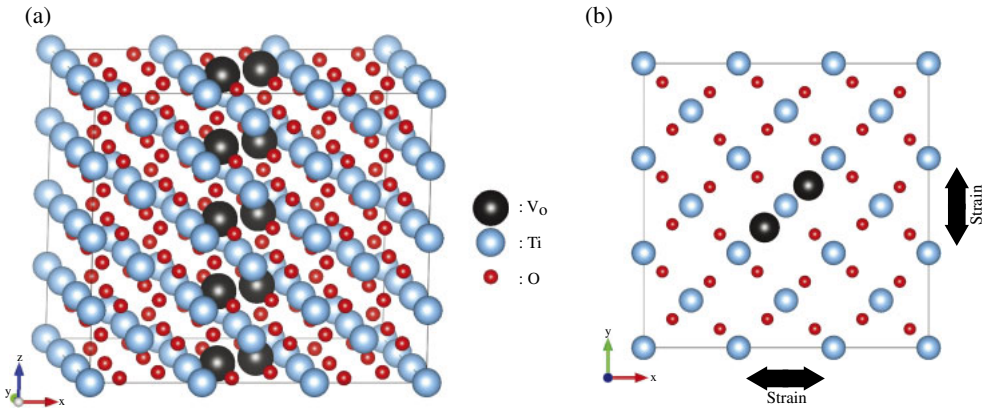

Fig. 2. (Color online) (a) Crystal structure of a 3×3×4 TiO_{2-x} supercell containing eight oxygen vacancies along the [001] direction. (b) Crystal structure of a 3×3×4 TiO_{2-x} supercell viewed along the (001) direction.

where the screening parameter μ defines the range separation and is set to 0.2 Å (HSE06 scheme) for both the HF and the DFT parts.[30] $E_x^{DFT,SR}$ is a density functional for the short-range part of the exchange energy, $E_x^{HF,SR}(\mu)$, is the exact nonlocal exchange evaluated with a screened Coulomb kernel, and E_C^{DFT} is the DFT correlation energy.

The ordered oxygen vacancies were introduced along the [001] direction within the 3×3×4 supercell of rutile TiO_{2-x} so that it consisted of 72 Ti and 136 O atoms. On-site Coulomb correction was applied the p orbital electrons (U^p) of O and d orbital electrons (U^d) of Ti. Park *et al.* optimized the parameters various p orbital and d orbital electrons ranging from 3 to 9 eV. We used 6 and 8 eV for p orbital and d orbital electrons, and 0.6 eV was used for the exchange (J) parameter.[8,14]

Another important elastic property is the Poisson ratio for uniaxial strain stress along the perpendicular of the x–y plane. Near the equilibrium structure, the Poisson ratio by DFT was in good agreement with experimental values.[31] Thus, we applied the Poisson ratio of 0.281 with external strain effect. In a typical simulation, two-dimensional-planar lattice strains of up to ±5% are imposed by lengthening and shortening the 3×3×4 TiO_2 supercell in the x- and y-directions.

3. Results and Discussion

We first performed *ab initio* calculations for rutile TiO_2 unit cells to validate the accuracy of the atomic structure data and the electronic structure data by comparing it to previous calculations. As mentioned above, conventional DFT is known to underestimate band gap energies for many oxides. In the case of TiO_2, the LDA+U calculation did not give the correct electronic structure if only the U^d correction was considered. According to Park *et al.*, the addition of Coulomb corrections for both 3d orbital electrons and 2p orbital electrons provides an improved description of the electronic properties.[8] Here, we used $a = 4.532$ and $c = 2.986$ for lattice parameters optimized by previous LDA+U^p+U^d research.[8]

The electronic structure of TiO_2 is illustrated in Figs. 1(a) and 1(b). The Fermi-level position was set to 0 eV. All the band states around the band gap largely consisted of O 2p states, hybridized with Ti 3d orbitals. The valance-band states were dominated by O 2p states, and the conduction-band states were mainly composed of Ti 3d states with small O 2p states. The conduction band was divided into two orbitals due to crystal field splitting. There were no significant differences in the electronic structures obtained with the LDA+U^p+U^d and the HSE06. The calculated band gap was around 3.0 eV for both LDA+U^p+U^d and HSE06, and it was in good agreement with the experiment results.

In Fig. 2(a), the schematic picture of the ordered oxygen vacancy configuration of TiO_2 is presented. The arrange-

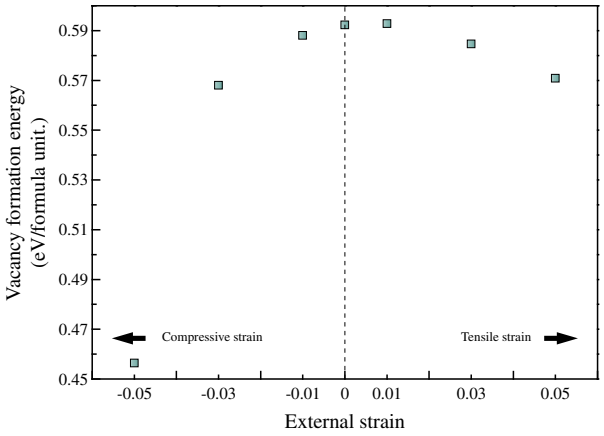

Fig. 3. (Color online) The ordered oxygen vacancies formation energies under external strains up to ±5%.

ment was located along the [001] direction. Figure 2(b) shows that the biaxial strain was applied in the *x*- and *y*-direction by rescaling the lattice parameters.

It is well known that oxygen vacancy make important effects to the electrical conductivity of TiO_2. The structure of the ordered oxygen vacancies showed a more stable than that of randomly distributed vacancies.[14] With this result, the stability of the ordered oxygen vacancy structures was investigated by comparing its oxygen vacancy formation energy under different biaxial strains of up to ±5%. The ordered oxygen vacancy formation energy, E_{vf}, serves as a measure of the strain response of oxygen defect chemistry. E_{vf} was calculated for biaxial lattice strains from −0.05 to 0.05. E_{vf} was calculated as

$$E_{vf} = E(TiO_{2-x}) - E(TiO_2) + n\mu_O, \quad (2)$$

where $E(TiO_{2-x})$ is the total energy of a supercell with the ordered oxygen vacancies, $E(TiO_2)$ is the total energy of a perfect TiO_2, μ_O is the oxygen chemical potential, and n is the number of oxygen vacancies. With LDA+U^d+U^p, the calculated single oxygen vacancy formation energy is 5.65 eV. This value is slightly higher than the experimental results of 4.55 and 4.57 eV.[32,33] In contrast, the formation energy of oxygen vacancy is lower than the other LDA+U method resulting in 6.37 and 6.03 eV.[8,34] As shown in Fig. 3, formation energies of the ordered oxygen vacancies are calculated as a function of the applied biaxial strains up to ±5%. Both compressive and tensile strain lowers the vacancy formation energy except in the case of 1% tensile strain. The formation energies slightly decreased when tensile strain increased, whereas compressive strain reduced the formation energies rapidly. The lowest formation energy was observed in the case of 5% compressive strain.

Figures 4(a) and 4(b) show the partial charge density corresponding to the defect state between Ti and Ti ions along the [001] direction. The defect-assisted tunneling through the metallic Ti ions is significant in the conduction mechanism of TiO_2.[14] In the cases of both Figs. 4(a) and 4(b), defect states near Ti ions were introduced as a conductive channel. Therefore, actual electron transport can be generated due to an oxygen vacancy chain in strain-induced TiO_2.

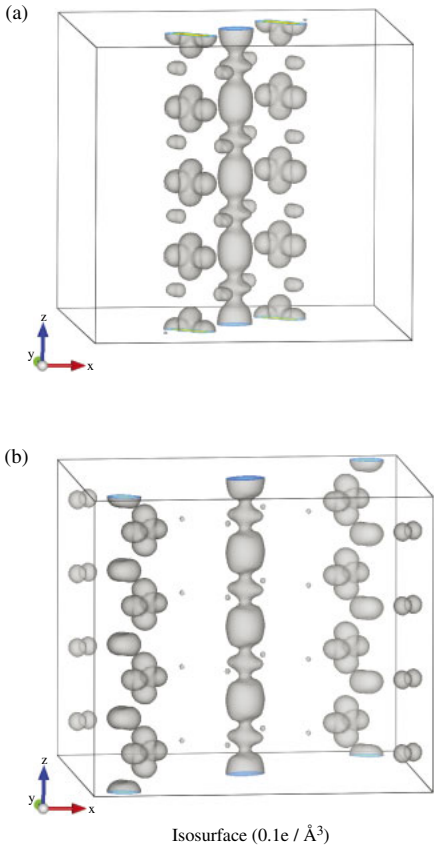

Fig. 4. (Color online) Band decomposed charge density of all defect states (a) with 5% compressive strain and (b) without strain.

4. Conclusions

In order to identify the formation energy of an oxygen vacancy chain with a strain effect, we performed first-principle LDA calculations. These calculations had on-site Coulomb corrections between O 2p orbital and Ti 3d orbital for TiO_2 and contained oxygen vacancies with external strain up to ±5%. The electronic structure of a unit cell using LDA+U^d+U^p corresponded with the hybrid functional electronic structure. The calculated single oxygen vacancy formation energy was 5.65 eV, which was close to the value from experiment results. As the strain increased up to ±5%, the formation energy of the ordered oxygen vacancies decreased. In particular, a 5% compressive strain was found to be the most favorable structure.

Based on the results, we believe that forming conductive filaments of TiO_2 can be controlled by applying external strain. The present results are valuable for the explanation of the resistance switching mechanism of TiO_2 ReRAM.

Acknowledgments

This work was supported by the National Research Foundation (NRF) grant funded by the Korea government (MEST, No. 2011-0016945) and Basic Science Research Program through the National Research Foundation of Korea (NRF) funded by the Ministry of Education, Science and Technology (No. 2011-0026175).

1) K. Tsunoda, Y. Fukuzumi, J. R. Jameson, Z. Wang, P. B. Griffin, and Y. Nishi: Appl. Phys. Lett. **90** (2007) 113501.
2) S. Seo, M. J. Lee, D. H. Seo, E. J. Jeoung, D.-S. Suh, Y. S. Joung, I. K. Yoo, I. R. Hwang, S. H. Kim, I. S. Byun, J.-S. Kim, J. S. Choi, and B. H. Park: Appl. Phys. Lett. **85** (2004) 5655.
3) T. W. Hickmott: J. Appl. Phys. **33** (1962) 2669.
4) Y. Watanabe, J. G. Bednorz, A. Bietsch, C. Gerber, D. Widmer, A. Beck, and S. J. Wind: Appl. Phys. Lett. **78** (2001) 3738.
5) A. Baikalov, Y. Q. Wang, B. Shen, B. Lorenz, S. Tsui, Y. Y. Sun, Y. Y. Xue, and C. W. Chu: Appl. Phys. Lett. **83** (2003) 957.
6) T. Sakamoto, H. Sunamura, H. Kawaura, T. Hasegawa, T. Nakayama, and M. Aono: Appl. Phys. Lett. **82** (2003) 3032.
7) J. J. Yang, M. D. Pickett, X. Li, D. A. A. Ohlberg, D. R. Stewart, and R. S. Williams: Nat. Nanotechnol. **3** (2008) 429.
8) S.-G. Park, B. Magyari-Kope, and Y. Nishi: Phys. Rev. B **82** (2010) 115109.
9) A. Chen, S. Haddad, Y. C. Wu, Z. Lan, T. N. Fang, and S. Kaza: Appl. Phys. Lett. **91** (2007) 123517.
10) D. C. Kim, S. Seo, S. E. Ahn, D. S. Suh, M. J. Lee, B. H. Park, I. K. Yoo, I. G. Baek, H. J. Kim, E. K. Yim, J. E. Lee, S. O. Park, H. S. Kim, U.-I. Chung, J. T. Moon, and B. I. Ryu: Appl. Phys. Lett. **88** (2006) 202102.
11) T. Fujii, M. Kawasaki, A. Sawa, H. Akoh, Y. Kawazoe, and Y. Tokura: Appl. Phys. Lett. **86** (2004) 012107.
12) X. Guo, C. Schindler, S. Menzel, and R. Waser: Appl. Phys. Lett. **91** (2007) 133513.
13) D.-H. Kwon, K. M. Kim, J. H. Jang, J. M. Jeon, M. H. Lee, G. H. Kim, X.-S. Li, G.-S. Park, B. Lee, S. Han, M. Kim, and C. S. Hwang: Nat. Nanotechnol. **5** (2010) 148.
14) S.-G. Park, B. Magyari-Kope, and Y. Nishi: IEEE Electron Device Lett. **32** (2011) 197.
15) B. Yang, F. Liu, and M. G. Lagally: Phys. Rev. Lett. **92** (2004) 025502.
16) G. H. Lu, M. Cuma, and F. Liu: Phys. Rev. B **72** (2005) 125415.
17) D.-J. Shu, S.-T. Ge, M. Wang, and N.-B. Ming: Phys. Rev. Lett. **101** (2008) 116102.
18) Z.-W. Wang, D.-J. Shu, M. Wang, and N.-B. Ming: Surf. Sci. **606** (2012) 186.
19) W. J. Yin, S. Y. Chen, J. H. Yang, X. G. Gong, Y. F. Yan, and S. H. Wei: Appl. Phys. Lett. **96** (2010) 221901.
20) L. Thulin and J. Guerra: Phys. Rev. B **77** (2008) 195112.
21) P. Rinke, A. Janotti, M. Scheffler, and C. G. Van de Walle: Phys. Rev. Lett. **102** (2009) 026402.
22) P. Rinke, A. Qteish, J. Neugebauer, and M. Scheffler: Phys. Status Solidi B **245** (2008) 929.
23) A. I. Liechtenstein, V. I. Anisimov, and J. Zaane: Phys. Rev. B **52** (1995) R5467.
24) G. Kresse and J. Hafner: Phys. Rev. B **47** (1993) 558.
25) G. Kresse and J. Joubert: Phys. Rev. B **59** (1999) 1758.
26) H. Hellmann: *Einfuhrung in die Quantumchemie* (Deuicke, Leipzig, 1937) p. 1 [in German].
27) M. J. Gillan: J. Phys.: Condens. Matter **1** (1989) 689.
28) H. J. Monkhorst and J. D. Pack: Phys. Rev. B **13** (1976) 5188.
29) J. Heyd, G. E. Scuseria, and M. Ernzerhof: J. Chem. Phys. **118** (2003) 8207.
30) A. V. Krukau, O. A. Vydrov, A. F. Izmaylov, and G. E. Scuseria: J. Chem. Phys. **125** (2006) 224106.
31) K. M. Glassford and J. R. Chelikoswsky: Phys. Rev. B **46** (1992) 1284.
32) P. Kofstad: *Nonstoichometry, Diffusion, and Electrical Conductivity in Binary Metal Oxides* (Wiley, New York, 1972) Chap. 8.
33) J. F. Marucco, J. Gautron, and P. Lemasson: J. Phys. Chem. Solids **42** (1981) 363.
34) K. Hameeuw, G. Cantele, D. Ninno, F. Trani, and G. Iadonisi: Phys. Status Solidi A **203** (2006) 2219.